

# Low-temperature enantiotropic $k2$ phase transition in the ionic 222-cryptand complex with $\text{LiClO}_4$

Ilia A. Guzei,<sup>a\*</sup> Lara C. Spencer,<sup>a</sup>  
Joe W. Su<sup>b</sup> and Ronald R.  
Burnette<sup>b</sup>

<sup>a</sup>Chemistry Department, University of  
Wisconsin–Madison, WI 53706, USA, and

<sup>b</sup>School of Pharmacy, University of Wisconsin–  
Madison, WI 53705, USA

Correspondence e-mail: iguzei@chem.wisc.edu

Received 6 September 2006

Accepted 26 October 2006

Crystallographic analyses at 100 and 200 K are reported for the macrobicyclic polyether 4,7,13,16,21,24-hexaoxa-1,10-diaza-bicyclo[8.8.8]hexacosane (denoted as 222-cryptand) that encapsulates a  $\text{Li}^+$  cation and then forms a complex (I) with  $\text{ClO}_4^-$ . Compound (I) undergoes a reversible second-order  $k$  phase transition at 253 (2) K from an almost ordered structure [space group  $P2_12_12_1$ ] at 100 K to a more disordered structure that exhibits a different unit cell [ $P2_12_12$  ( $2c' = c$ )] above 253 (2) K. At 295 K the  $\text{Li}^+$  cation and five atoms of the perchlorate anion are each disordered over at least two positions about a crystallographic twofold axis [Chekhlov (2003). *Russ. J. Coord. Chem.* **29**, 828–832]; as the temperature decreases the dynamic positional disorder is slowly frozen out, but is still observed for lithium even at 100 K. Based upon DFT computations, it seems that in the solid state the position of the  $\text{Li}^+$  cation in the cavity of the 222-cryptand below 253 (2) K likely corresponds to a local energy minimum; the global minimum in the gas phase corresponds to a near  $D_3$  symmetrical conformation of the 222-cryptand with the undersized  $\text{Li}^+$  cation residing in the center of its cavity.

## 1. Introduction

The well known macrobicyclic polyether 4,7,13,16,21,24-hexaoxa-1,10-diaza-bicyclo[8.8.8]hexacosane (222-cryptand) belongs to a class of ligand carriers that possess strong affinities for alkali and alkaline earth cations, as noted by their creators Lehn & Sauvage (1971). Wide-ranging applications of cryptands include their use as radionuclide decorporating agents (Varga *et al.*, 1994), as model systems for understanding the mechanism of ionophoric action (Lamb *et al.*, 1980, 1981; Riddell, 1992) and as cation/counterion separation agents (Chiou & Shih, 1996).

More recently, computational efforts have been directed towards the conformational understanding of these systems in water (Auffinger & Wipff, 1991), acetonitrile (Troxler & Wipff, 1994) and the water–chloroform interface (Jost *et al.*, 2002). These studies utilize molecular mechanics/dynamics software such as *AMBER* (Cornell *et al.*, 1995), which requires empirical force-field parameterization derived from *ab initio* calculations. To ensure accurate computational analysis, experimental benchmarks based upon crystal structures are necessary.

Crystal structures involving the 222-cryptand macrocycle have been reported for the uncomplexed form (Metz *et al.*, 1976), and the KI (Moras & Weiss, 1973*a*), NaI (Moras & Weiss, 1973*b*) and  $\text{LiClO}_4$  (Chekhlov, 2003) salt complexes. As a first step in our investigation of the temperature dependence of the cation behavior inside the cavity of the 222-cryptand, we isolated crystals of 222-cryptand/ $\text{LiClO}_4$  (I), in which the

cation and anion exhibit positional disorder at 295 K, as reported by Chekhlov (2003).

There are many examples in the literature of order–disorder phase transitions which result in the doubling of the unit cell at lower temperature. Compounds which undergo phase transitions where the volume of the unit cell doubles but the space group remains unchanged include organic kinetin dihydrogen phosphate (Slosarek *et al.*, 2006) and organometallic compounds such as *catena*-[( $\mu$ - $\eta^3$ -toluene)-bis[caesium(2,4,6-tri-*tert*-butylphenylphosphide)]] (Concolino *et al.*, 2000) and tetraallyl (2,2'-bipyridyl)-*rac*-3,3,7,7-tetramethyl-*trans*-5-palladatricyclo-[4.1.0.0<sub>2,4</sub>]heptane-1,2,4,6-tetracarboxylate (Bats *et al.*, 2000). Each of their crystal structures belongs to the triclinic space group  $P\bar{1}$ . There are numerous examples of phase transitions where the doubling of the unit-cell volume results in a change in the crystal system and space group, as exemplified by tetramethylammonium perchlorate which at 210 K has the tetragonal unit cell (space group  $P4/nmm$ ), but at 150 K undergoes a transition to an orthorhombic unit cell (space group  $P2_12_12_1$ ) with twice the volume (Palacios *et al.*, 2003). Other phase transitions of mainly organic compounds give rise to the conversion of a mirror plane into a glide plane at lower temperature; examples are nitroimidazole derivatives which transform from the monoclinic  $P2_1/m$  symmetry at 295 K to monoclinic  $P2_1/c$  symmetry at 200 K with a simultaneous doubling of the unit cell volume (Kubicki, 2004).

Presented herein are the results of our detailed low-temperature study of complex (I) which was observed to transform from an orthorhombic cell of  $P2_12_12_1$  symmetry initially determined by Chekhlov at 295 K to  $P2_12_12_1$  symmetry below 253 (2) K; the transformation features the twofold rotation axis in the *c* direction becoming a  $2_1$  screw axis with a concomitant doubling of the *c* axis length. Noteworthy is that this particular space-group change, which is similar to the above examples involving a mirror becoming a glide plane, has not been previously reported (to the knowledge of the authors). This investigation has provided detailed information concerning the temperature dependence of the position of the  $\text{Li}^+$  cation encapsulated within the oversized cavity of the 222-cryptand.

## 2. Experimental

### 2.1. Sample preparation

Compound (I), a 1:1 222-cryptand/ $\text{LiClO}_4$  complex, was prepared as described in previous work (Chekhlov, 2003). An equimolar mixture of 222-cryptand and  $\text{LiClO}_4$  was prepared in acetone. The mixture was then allowed to evaporate at a slow rate until crystallization was observed.

### 2.2. Structure determination

Crystal structure determinations of (I) at 100 and 200 K were performed in a typical fashion using a platform CCD diffractometer. During the structural refinement of (I) at 200 K geometrical restraints were imposed on the disordered

perchlorate anion to ensure its tetrahedral shape and the computational stability of the refinement.

### 2.3. Cell-dimension measurements

The unit-cell dimensions and the number of reflections for unit-cell determination were measured in the heating regimen at 10 K intervals over the range 100–300 K, with the standard matrix determination routine with three sets of 20  $0.3^\circ$  scans and an exposure time of 10 s per frame, and in 4 K increments over the range 240–260 K, with three sets of 20  $0.3^\circ$  scans and an exposure time of 60 s per frame. The 4 K increments were narrowed further to elucidate the exact transition temperature of 253 (2) K. The reflections were indexed by the use of the program *CELL\_NOW* (Sheldrick, 2005) and the unit-cell parameters refined with a non-linear least-squares routine in *SMART* (Bruker, 2003). *CELL\_NOW* unambiguously indexed reflections for temperatures outside the 240–260 K temperature range; within the range *CELL\_NOW* would usually suggest the smaller cell as its primary choice and, if chosen, the unit cell would correspond to the major component of a twinned crystal with at least two more minor components that would or would not be related to the major component by a sensible symmetry transformation. Manually forcing the program to index the reflections to produce the larger unit cell resulted in all reflections being indexed as belonging to one domain with the reflections *hkl* with *l* = odd also present.

A differential scanning calorimetry experiment was conducted with 20 mg of crystals of (I) in the 10 and  $5^\circ \text{min}^{-1}$  heating regimen between 110 and 295 K. It was determined that the phase transition begins at 253.5 K and is completed at 261.9 with the transition temperature being 257.6 K (see Fig. 1).

## 3. Results and discussion

### 3.1. Phase transition

Compound (I) undergoes a solid-state enantiotropic *k2* phase transition at approximately 253 (2) K. Type *k2* was established as follows. Type *k* was assigned because during the phase transition the crystal class and system remain

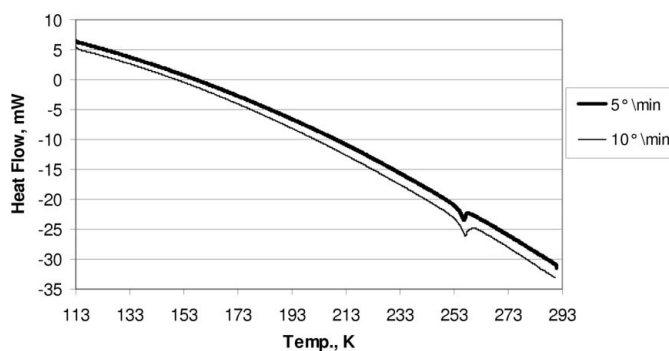


**Figure 1**  
The DSC measurement of (I). The upper curve corresponds to the heating rate of  $5 \text{ K min}^{-1}$ , the lower to  $10 \text{ K min}^{-1}$ .

**Table 1**

Experimental details.

NR = not reported by Chekhlov (2003).

	(I)	(I)	(I) (Chekhlov, 2003)
Temperature (K)	100 (2)	200 (2)	295
Chemical formula	C <sub>18</sub> H <sub>36</sub> LiN <sub>2</sub> O <sub>6</sub> ·ClO <sub>4</sub>	C <sub>18</sub> H <sub>36</sub> LiN <sub>2</sub> O <sub>6</sub> ·ClO <sub>4</sub>	C <sub>18</sub> H <sub>36</sub> LiN <sub>2</sub> O <sub>6</sub> ·ClO <sub>4</sub>
<i>M<sub>r</sub></i>	482.88	482.88	482.88
Wavelength (Å)	0.71073	0.71073	0.71073
Cell setting, space group	Orthorhombic, <i>P</i> <sub>2</sub> <sub>1</sub> <sub>2</sub> <sub>1</sub>	Orthorhombic, <i>P</i> <sub>2</sub> <sub>1</sub> <sub>2</sub> <sub>1</sub>	Orthorhombic, <i>P</i> <sub>2</sub> <sub>1</sub> <sub>2</sub> <sub>1</sub>
<i>a</i> , <i>b</i> , <i>c</i> (Å)	10.0273 (7), 13.3313 (9), 16.8827 (12)	10.0791 (5), 13.3799 (6), 17.0272 (8)	10.149 (2), 13.475 (3), 8.580 (1)
<i>V</i> (Å <sup>3</sup> )	2256.8 (3)	2296.24 (19)	1173.4 (4)
<i>Z</i>	4	4	2
<i>D<sub>x</sub></i> (Mg m <sup>-3</sup> )	1.421	1.397	1.367
<i>μ</i> (mm <sup>-1</sup> )	0.23	0.22	0.22
Crystal form, color	Block, colorless	Block, colorless	Block, colorless
<i>F</i> (000)	1032	1032	1032
Crystal size (mm)	0.48 × 0.41 × 0.37	0.48 × 0.41 × 0.37	0.55 × 0.45 × 0.40
<b>Data collection</b>			
Diffractometer	Bruker CCD-1000 area detector	Bruker CCD-1000 area detector	Enraf–Nonius CAD-4
Data collection method	0.30° <i>ω</i> scans	0.30° <i>ω</i> scans	NR
Absorption correction	Multi-scan (based on symmetry-related measurements)	Multi-scan (based on symmetry-related measurements)	NR
<i>T<sub>min</sub></i>	0.899	0.901	NR
<i>T<sub>max</sub></i>	0.921	0.922	NR
No. of measured, independent and observed reflections	26 669, 4621, 4504	26 861, 4697, 4544	2330, 2312, 1750
Criterion for observed reflections	<i>I</i> > 2σ( <i>I</i> )	<i>I</i> > 2σ( <i>I</i> )	<i>I</i> > 2σ( <i>I</i> )
<i>R<sub>int</sub></i>	0.041	0.025	NR
Theta range for data collection (°)	2.35–26.39	2.35–26.39	≤ 32
Completeness to θ = 26.38° (%)	100	99.9	NR
<b>Refinement</b>			
Refinement on	<i>F</i> <sup>2</sup>	<i>F</i> <sup>2</sup>	<i>F</i> <sup>2</sup>
<i>R</i> [ <i>F</i> <sup>2</sup> > 2σ( <i>F</i> <sup>2</sup> )], <i>wR</i> ( <i>F</i> <sup>2</sup> ), <i>S</i>	0.026, 0.072, 1.07	0.031, 0.089, 1.08	0.042, 0.112, 1.03
No. of reflections	4621	4697	NR
No. of parameters	289	327	NR
H-atom treatment	Constrained to parent site	Constrained to parent site	NR
Weighting scheme	<i>w</i> = 1/[σ <sup>2</sup> ( <i>F<sub>o</sub></i> <sup>2</sup> ) + (0.0395 <i>P</i> ) <sup>2</sup> + 0.5245 <i>P</i> ], where <i>P</i> = ( <i>F<sub>o</sub></i> <sup>2</sup> + 2 <i>F<sub>c</sub></i> <sup>2</sup> )/3	<i>w</i> = 1/[σ <sup>2</sup> ( <i>F<sub>o</sub></i> <sup>2</sup> ) + (0.0553 <i>P</i> ) <sup>2</sup> + 0.3192 <i>P</i> ], where <i>P</i> = ( <i>F<sub>o</sub></i> <sup>2</sup> + 2 <i>F<sub>c</sub></i> <sup>2</sup> )/3	NR
(Δ/σ) <sub>max</sub>	0.001	0.002	0.001
Δρ <sub>max</sub> , Δρ <sub>min</sub> (e Å <sup>-3</sup> )	0.21, -0.39	0.25, -0.21	0.14, -0.14
Absolute structure	Flack (1983)	Flack (1983)	Flack (1983)
Flack parameter	-0.03 (4)	-0.03 (5)	0.03 (9)

Computer programs used: SMART, SAINT, SHELXTL (Bruker, 2003).

unchanged; specifically, the space group *P*<sub>2</sub><sub>1</sub><sub>2</sub><sub>1</sub> observed below 253 (2) K is transformed to its *k* minimal non-isomorphic supergroup II *P*<sub>2</sub><sub>1</sub><sub>2</sub><sub>1</sub><sub>2</sub> (2*c*' = *c*) observed above 253 (2) K. The transition is presumed to be second order, since it gradually occurs over a range of temperatures. Evidence for a second-order transformation is provided by the number of observed reflections used for the determination of the unit cell size between 100 and 300 K (Fig. 2). The number of reflections for the larger unit cell with *P*<sub>2</sub><sub>1</sub><sub>2</sub><sub>1</sub> symmetry should ideally be nearly twice the number of reflections for a cell with *P*<sub>2</sub><sub>1</sub><sub>2</sub><sub>1</sub><sub>2</sub> (2*c*' = *c*) symmetry. Our data show that at 100 K the number of reflections exceeds those at 295 K by more than a factor of two owing to the theoretically larger number of reflections and their higher intensity, which allowed more reflections to be selected for the matrix determination routine. The number of reflections remained roughly the same between 100 and 150 K, but upon elevation of the temperature from 150 to 250 K the number of selected reflections gradually diminished and then

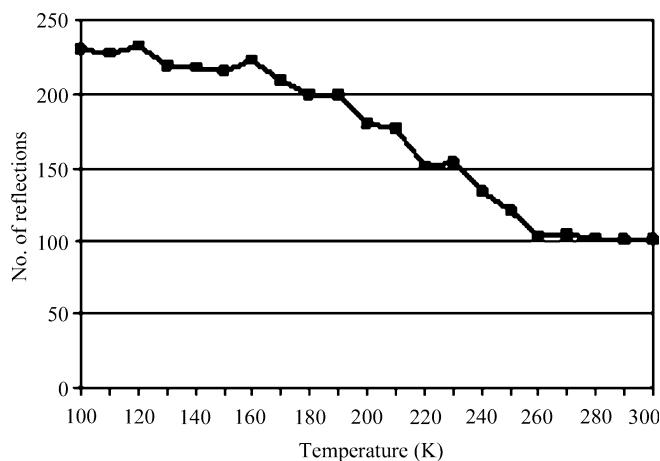


**Figure 2**  
Temperature dependence of the number of reflections used for the unit-cell determination of (I).

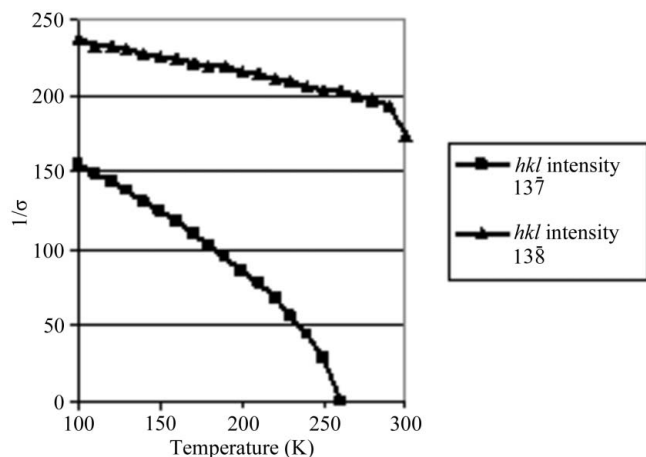
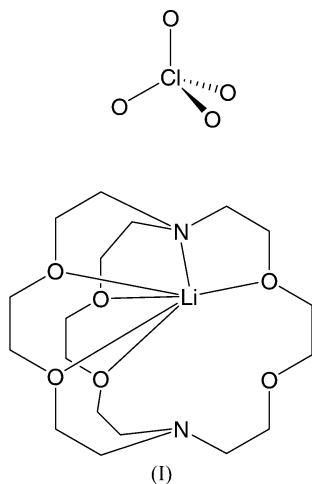


**Figure 3**  
Temperature dependence of intensities of the  $hkl$  reflections  $13\bar{7}$  ( $l = \text{odd}$ ) and  $13\bar{8}$  ( $l = \text{even}$ ) for (I). The  $13\bar{7}$  reflection disappears at 253 K, as the  $c$ -axis length is halved in size.

plateaued at  $\sim 260$  K. Observed changes in the intensities were found to be different for  $hkl$  reflections with  $l = \text{even}$  versus those with  $l = \text{odd}$ ; intensities of the latter decreased more rapidly as the temperature was raised (Fig. 3), totally disappearing above 253 (2) K.



The volume of the unit cell [ $2256.8(2) \text{ \AA}^3$ ] increased slightly as the temperature was incremented from 100 K to the transition at 253 (2) K presumably owing to the increased atomic thermal motion (Fig. 4). As the phase transition occurred the cell volume was reduced to half its previous size. Upon further heating of the system the cell volume once again increased slightly owing to the thermal expansion to  $1173.4(4) \text{ \AA}^3$  at 295 K (Table 1)<sup>1</sup> (Chekhlov, 2003). All cell parameters have positive expansion coefficients with a discontinuity observed for the  $c$  axis (Fig. 5). Concomitantly, the  $Z'$  value transforms from 1 at 100 K to 0.5 at 295 K and the ordered cryptand

<sup>1</sup> Supplementary data for this paper are available from the IUCr electronic archives (Reference: AV5077). Services for accessing these data are described at the back of the journal.

ligand now resides on a crystallographic twofold axis while the lithium and perchlorate ions are disordered over twofold axes. During the transition the twofold screw axis along the  $c$  axis upgrades to a proper twofold axis.

### 3.2. Crystal disorder

Originally, when only X-ray data for 100 and 295 K were available, we classified the transition as order(100 K)–disorder(295 K). However, a subsequent analysis of the X-ray data collected at 200 K indicated the transition may be better described as ‘less disorder of the lithium and perchlorate ions (100 K) – at least 1:1 disorder of the lithium and perchlorate ions (295 K)’. The positional disorder observed throughout the experimental temperature range is dynamic in nature. We propose that subtle intermolecular packing interactions constitute the driving force for the perchlorate disorder and that electrostatic interactions within the 222-cryptand macrocycle account for the lithium disorder (Fig. 6).

The nature of the lithium disorder is more interesting and it is also better understood. In order to gain insight into the

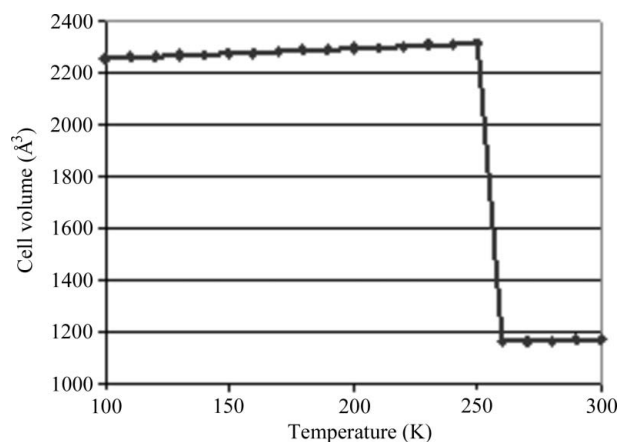


**Figure 4**  
Temperature dependence of the unit-cell volume of (I).

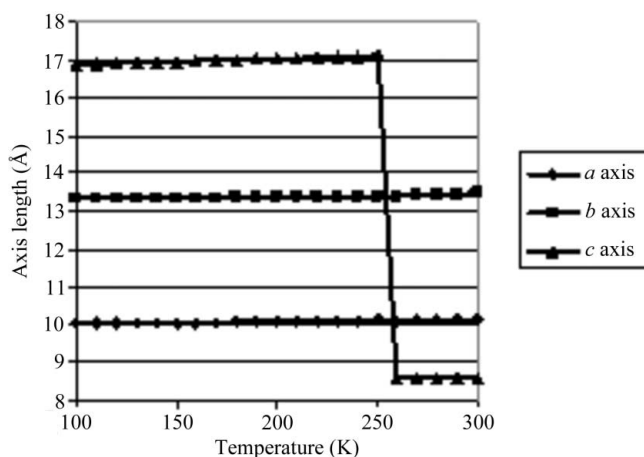


**Figure 5**  
Temperature dependence of the unit-cell axes of (I).

disorder in this system we acquired complete data sets at 100 and 200 K and herein compare them with the data set acquired at 295 K by Chekhlov. In the structure of (I) at 100 K there appears to be no disorder in the positions of the perchlorate and macrocycle atoms, while the  $\text{Li}^+$  cation remains somewhat thermally mobile, as judged from the shape of its slightly enlarged anisotropic thermal ellipsoid (Fig. 7). The principal axis of this lithium thermal ellipsoid is directed between triangles formed by atoms N1–O1–O5 and N2–O4–O2 rather than between the two N atoms alone. This description is consistent with the disorder observed at 200 and 295 K. It is believed that the undersized  $\text{Li}^+$  cation has still not found the optimal site even at 100 K and a lower temperature is required to minimize its thermal motion, but such an investigation was outside the scope of this study. As the temperature is increased, the atomic thermal motion expectedly increases and at 200 K the lithium thermal ellipsoid becomes more elongated: the ratio of the largest and smallest principal mean-square atomic displacements  $U$  for Li1 is 2.87 at 100 K and 4.08 at 200 K. At 200 K the O atoms of the perchlorate anion are no longer satisfactorily described as each residing at one site. A refinement with their indicated disorder in a 3:1 ratio modelled with appropriate restraints improved the overall refinement and lowered the  $R$  factor from 0.0471 to 0.0306. At 253 (2) K the phase transition takes place, whereas above this temperature the cation and all five atoms of the perchlorate are disordered over crystallographic twofold axes, while the

222-cryptand remains ordered but now exhibits  $C_2$  symmetry, (Fig. 6). The  $\text{Li}^+$  cation is equally disordered about a twofold axis occupying the major sites separated by 0.52 (1) Å at 295 K (Chekhlov, 2003; see Fig. 8).

Dynamic positional disorder of the Li atom is present throughout the experimental temperature range. The perchlorate atoms are ordered at 100 K, but exhibit progressively more disorder at the higher temperatures. Since the perchlorate contains the heaviest diffractors in this system its crystal disorder significantly contributes to the lowering of the reflection intensities (Fig. 2). According to this graph, the disorder of the perchlorate anion becomes noticeable at  $\sim 150$ – $160$  K, reaches 25% at 200 K and is essentially completed at 253 (2) K. Above this temperature, the behavior of the perchlorate is best described as a sphere of smeared electron density formed by the O atoms. In the lattice of (I) the perchlorate with an approximate volume of  $\sim 67$  Å<sup>3</sup> occupies a solvent accessible void of  $\sim 87$  Å<sup>3</sup> (computed by conventional methods with *PLATON*; Spek, 2003) and has therefore sufficient freedom to tilt and rotate among many energetically comparable positions in the solid state. On the other hand, the  $\text{Li}^+$  disorder is not as multipositional as that of the perchlorate O atoms in that the small lithium cation is encapsulated within a cavity whose shape remains more or less intact. Above the transition temperature the lithium cation has no preference between the two distinct equivalent positions, but below 253 (2) K it occupies only one of them and thus the twofold rotation axis disappears.

It would be interesting to evaluate the energy of the phase transition in this system, but unfortunately there is no reliable method of deriving such information from the crystallographic data. Therefore, only the lithium disorder was investigated by means of DFT calculations at the b3lyp/6-31G\* and b3lyp/6-31+G\* level of theory with *GAUSSIAN03* (Frisch *et al.*, 2003).

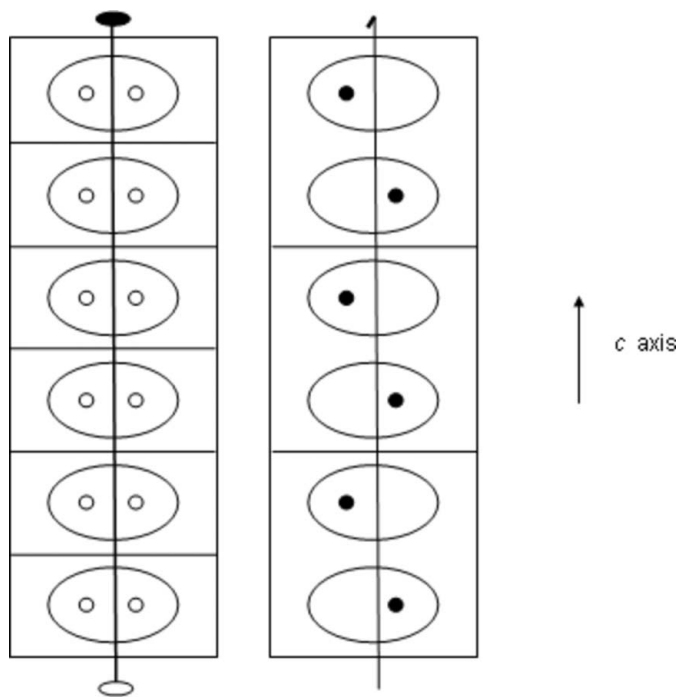


**Figure 6**

A schematic representation of the  $\text{Li}^+$  disorder in (I). The rectangles denote unit cells, ovals the 222-cryptand, open circles 50% occupied  $\text{Li}^+$  cations, and filled circles fully occupied  $\text{Li}^+$  cations. The twofold axis over which the  $\text{Li}^+$  cations are disordered above 253 (2) K (left) transforms into a twofold screw axis with a concomitant doubling of the cell volume below 253 (2) K (right).

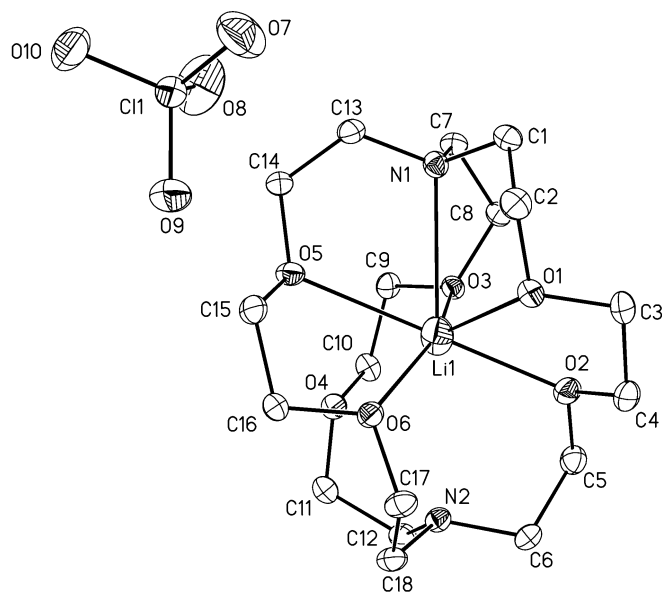


**Figure 7**

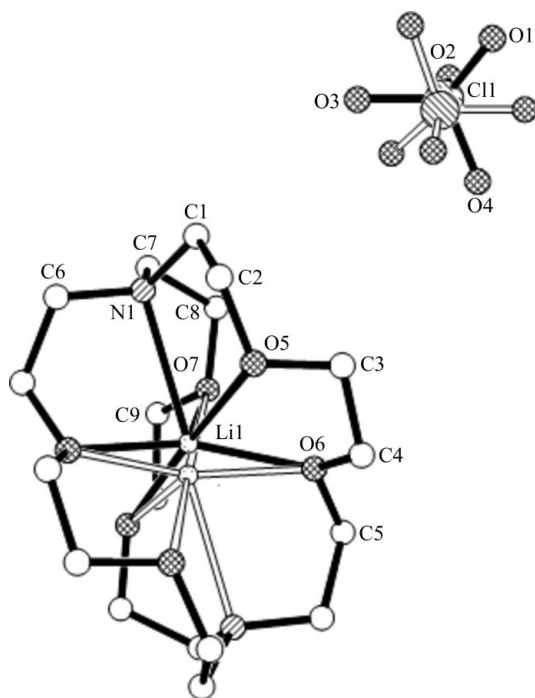
A molecular drawing (I) at 100 (2) K shown with 30% probability displacement ellipsoids. All H atoms are omitted for clarity.

**Table 2**  
 Selected interatomic distances in (I).

100 (2) K	<i>d</i> (Å)	295 K	<i>d</i> (Å)
Li1—N1	2.681 (3)	Li1—N1	2.592 (7)
Li1—O1	2.326 (3)	Li1—O7	2.252 (9)
Li1—O2	2.265 (3)	Li1—O7 <sup>i</sup>	2.507 (9)
Li1—O3	2.076 (3)	Li1—O6 <sup>i</sup>	2.054 (15)
Li1—O5	2.497 (3)	Li1—O5	2.577 (8)
Li1—O6	2.072 (3)	Li1—O6	2.088 (14)
Li1···O4	2.933 (3)	Li1···O5 <sup>i</sup>	2.867 (9)
Li1···N2	3.030 (3)	Li1···N1 <sup>i</sup>	3.091 (7)
N1···N2	5.7015 (16)	N1···N1 <sup>i</sup>	5.682 (3)

 Symmetry code: (i)  $-x, -y, z$ .

Three geometrical minimizations were performed to find the energy minima corresponding to the lithium positions at each of the two ‘disordered’ sites within the 222-cryptand reported by Chekhlov, and one for the energy maximum between the two. The experimental atomic coordinates were used as the starting points for the first two computations and a complex with an approximate  $D_3$  symmetry for the third. All minimizations converged to the same geometry in which the conformation of the 222-cryptand is almost  $D_3$  symmetrical. The lithium cation resides in the center of its cavity and is equidistant from the six O atoms and equidistant from the two N atoms. The lithium is bonded to all six O atoms, but to neither of the N atoms, which is a logical result based on the electrostatic considerations because the more electronegative O atoms are the better electron donors. We conclude that the experimentally observed site of the  $\text{Li}^+$  within the 222-cryp-


**Figure 8**  
 A ball-and-stick representation of (I) at 295 K based on the CSD data (Allen, 2002). All H atoms are omitted for clarity. The lithium and the  $\text{ClO}_4^-$  anion are disordered over two positions with a 1:1 ratio.

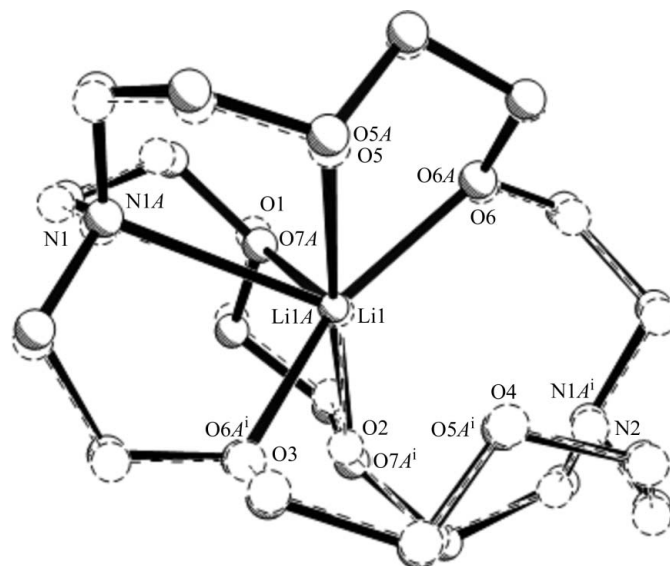
tand at 100 K either corresponds to a local energy minimum or to the global energy minimum in the solid state. In our computations no periodic boundary conditions were imposed. In the following discussion we will refer to the theoretically optimized structure of the 222-cryptand/ $\text{Li}^+$  as (I-DFT).

### 3.3. Bond comparison

A drawing of the asymmetric unit of (I) at 100 K is shown in Fig. 7 and a superimposition of structures of (I) determined at 100 and 295 K is presented in Fig. 9. Selected bond distances and angles are tabulated in Table 2.

The crystal structures of (I) at 100 and 295 K are similar (when only one position of the Li atom is considered for the latter), as Fig. 9 confirms. The respective Li–element bond distances compare well between the two structures and in both the lithium cation appears to be six-coordinate, bonding to one N and five O atoms.

The Li1—N1 distance in (I) at 100 K is substantially shorter than the other Li1—N2 separation. The distances between Li1 and N2 at 100 K of 3.030 (3) Å, and between Li1 and N1<sup>i</sup> [(i) =  $-x, -y, z$ ] at 295 K of 3.091 (7) Å (Chekhlov, 2003) are both much larger than the sum (2.31–2.47 Å) of the effective ionic radius of the  $\text{Li}^+$  cation (0.76 Å for a coordination number of six, 0.92 Å for a coordination number of eight; Shannon, 1976), and the van der Waals radius of the nitrogen (1.55 Å). Five O atoms coordinate to the Li1 cation with disparate distances ranging between 2.072 (3) and 2.497 (3) Å, but the Li1···O4 separation of 2.933 (3) Å at 100 K and the Li1—O5<sup>i</sup> [(i) =  $-x, -y, z$ ] of 2.867 (9) Å at 295 K (Chekhlov, 2003) substantially exceed the sum of the  $\text{Li}^+$  effective ionic radius and the van der Waals radius for oxygen (2.28–2.44 Å). The


**Figure 9**  
 Overlay diagram of (I) at 100 and 295 K with an r.m.s. deviation of 0.122 Å. All H atoms and the  $\text{ClO}_4^-$  anion are omitted for clarity. The dashed bonds correspond to the atomic positions of compound (I) at 100 K. All atoms with A suffixes correspond to the positions of compound (I) at 295 K. [Symmetry code: (i)  $-x, -y, z$ ]

**Table 3**

Comparison of complexes with different metal atoms.

	Li <sup>+</sup> 100 K	Li <sup>+</sup> 200 K	Na <sup>+</sup> (Metz <i>et al.</i> , 1971)	K <sup>+</sup> (Metz <i>et al.</i> , 1971)	Rb <sup>+</sup> (Metz <i>et al.</i> , 1971)	Cs <sup>+</sup> (Metz <i>et al.</i> , 1971)	Uncomplexed 222-cryptand (Metz <i>et al.</i> , 1976)
$\alpha$ (°)	53.9 (9)	53.4 (6)	45	21	15	15	N/A
N1...N2 (Å)	5.7015 (16)	5.6849 (18)	5.54	5.732	6.00	6.058	6.872

 $\alpha$  is defined by Metz *et al.* (1971).

Li1—O distances can be grouped in four categories – two strong bonds, two bonds of medium strength, one weak bond and one non-bonding separation.

In complex (I-DFT) all of the lithium–oxygen bond distances [average 2.366 (4) Å] correspond well to the sum of the Li<sup>+</sup> effective ionic radius and the oxygen van der Waals radius, indicating that in the optimized structure the O atoms approach the Li atoms more closely, forcing the N atoms farther away; the Li...N separations in (I-DFT) average 2.956 (4) Å. This is attributed to the fact that the more electronegative O atoms interact with the lithium cation stronger than the less electronegative N atoms.

### 3.4. Comparison to similar compounds with group I metals

The ionic diameter of Li<sup>+</sup> is 1.52 Å (Shannon, 1976) for a coordination number of six and 1.84 Å for a coordination number of eight, and both are significantly smaller than the 2.8 Å diameter void in the 222-cryptand in its optimal conformation (Table 3; Lehn & Sauvage, 1971). The ionic diameters of the other alkali metals Na<sup>+</sup>, K<sup>+</sup>, Rb<sup>+</sup> and Cs<sup>+</sup> are substantially larger at 2.36, 3.02, 3.22 and 3.48 Å, respectively. The lithium ion is too small to be within bonding distance of all eight heteroatoms of the ligand and therefore it only forms bonds with six. Lithium cation coordination to one N and five O atoms of a 222-cryptand has been previously observed in (222-cryptand-*N,O,O',O'',O''',O''''*)-lithium 1-methyl-2,3,6-triphenyl-1-phosphacyclohexa-2,4-dienide tetrahydrofuran solvate (Moores *et al.*, 2003) and (222-cryptand-*N,O,O',O'',O''',O''''*)-lithium 1-*tert*-butyl-3,5-diphenyl-2,6-bis-(trimethylsilyl)-1-phosphacyclohexa-2,4-dienide (Moores *et al.*, 2003), and two one N and arguably four O atoms in bis(222-cryptand-*N,O,O',O'',O''',O''''*)-lithium (*R,S,R,S*)-bis(1,2-diphenyl-1,2-bis(phenylphosphido)ethane-*P,P'*)platinum(II) (Tirla *et al.*, 2002). In contrast, larger ions such as sodium, potassium, rubidium and caesium fill the ligand cavity better and bond with all eight heteroatoms (Metz *et al.*, 1971). In such complexes the 222-cryptand heteroatoms form a bicapped trigonal prism of *D*<sub>3</sub> symmetry, whereas compound (I) has *C*<sub>1</sub> symmetry below 253 (2) K and *C*<sub>2</sub> symmetry above that temperature. In complexes with other metals and in complex (I-DFT), the two triangular faces formed by the O atoms located above and below the cation are parallel (Metz *et al.*, 1971). In compound (I) at 100 (2) K the planes form a dihedral angle of 9.94 (5)°. The value of the angle  $\alpha$  (Metz *et al.*, 1971) of the lateral twist between the two triangular faces defined by the O atoms (Table 3) is largest for the lithium complex (I) corresponding to the smallest metal incorporated

into the ligand. The  $\alpha$  angle progressively decreases as the metal diameter becomes larger, moving towards *D*<sub>3</sub> symmetry (Metz *et al.*, 1971).

It has been demonstrated that the complex with the potassium ion, whose ionic diameter is closest to the ligand void diameter, is the most stable (Lehn & Sauvage, 1971). The Na<sup>+</sup> ion, while larger than the lithium and thus able to bond with all eight ligand heteroatoms, is still too small to efficiently fill the cavity and the mean bond distances between the metal and the ligand are larger than the sum of the ionic radii of the sodium and the van der Waals radii of oxygen and nitrogen, indicating weak bonds at room temperature (Metz *et al.*, 1971). The Cs<sup>+</sup> ion is so large that there is steric repulsion between it and the ligand heteroatoms, forming a less stable complex than potassium, rubidium and sodium (Metz *et al.*, 1971).

## 4. Summary

We have discovered, studied and described a phase transition in the 222-cryptand/LiClO<sub>4</sub> system. A twofold rotation axis becomes a 2<sub>1</sub> screw axis with concomitant doubling of the axial length when the complex is cooled below the transition temperature of 253 (2) K. This transformation has been classified as a reversible *k*2 transition from the orthorhombic unit cell *P*2<sub>1</sub>2<sub>1</sub>2<sub>1</sub> observed below 253 (2) K to its *k* minimal non-isomorphic supergroup II *P*2<sub>1</sub>2<sub>1</sub>2 (2*c'* = *c*) above it. While the dynamic positional disorder of the lithium cation and perchlorate anion is reduced as the temperature is lowered, the anisotropic shape of the atomic ellipsoid of the Li<sup>+</sup> cation indicates its thermal mobility even at 100 K. DFT optimization calculations suggest that neither the low- nor high-temperature structure is in an optimal configuration. In the crystal structures of (I) at 100 and 295 K, the central lithium is bonded to one N atom and five O atoms, while in the DFT-optimized structure the lithium ion is bonded to the six O atoms and to neither of the N atoms. Both the structure and phase transition in the 222-cryptand/LiClO<sub>4</sub> system are presumably exceptional in that larger alkali metal ions would more completely occupy the ligand cavity and thereby form bonds to all eight heteroatoms.

We thank Dr Lingzhi Zhang (University of Wisconsin–Madison) for conducting the DSC experiment and Professor Larry Dahl (University of Wisconsin–Madison) and Professor Håkon Hope (University of California, Davis) for fruitful discussions of the project.

## References

- Allen, F. H. (2002). *Acta Cryst.* **B58**, 380–388.
- Auffinger, P. & Wipff, G. (1991). *J. Am. Chem. Soc.* **113**, 5976–5988.
- Bats, J. W., Nass, A. R. & Hashmi, A. S. K. (2000). *Acta Cryst.* **C56**, 814–817.
- Bruker (2003). *SADABS* (Version 2.05), *SAINT* (Version 6.22), *SHELXTL* (Version 6.10), *SMART* (Version 5.622). Bruker-AXS Inc., Madison, Wisconsin, USA.
- Chekhlov, A. N. (2003). *Russ. J. Coord. Chem.* **29**, 828–832.
- Chiou, C.-S. & Shih, J.-S. (1996). *Analyst*, **121**, 1107–1110.
- Concolino, T. E., Lam, K.-C., Guzei, I. A., Rheingold, A. L. & Rabe, G. W. (2000). *Acta Cryst.* **B56**, 210–214.
- Cornell, W. D., Cieplak, P., Bayly, C. I., Gould, I. R., Merz, K. M., Ferguson, D. M., Spellmeyer, D. C., Fox, T., Caldwell, J. W. & Kollman, P. A. (1995). *J. Am. Chem. Soc.* **117**, 5179–5197.
- Flack, H. D. (1983). *Acta Cryst.* **A39**, 876–881.
- Frisch, M. J. *et al.* (2003). *GAUSSIAN03*, Revision C.02. Gaussian, Inc., Wallingford, Connecticut, USA.
- Jost, P., Galand, N., Schurhammer, R. & Wipff, G. (2002). *Phys. Chem. Chem. Phys.* **4**, 335–344.
- Kubicki, M. (2004). *Acta Cryst.* **B60**, 333–342.
- Lamb, J. D., Christensen, J. J., Oscarson, J. L., Nielsen, B. L., Asay, B. W. & Izatt, R. M. (1980). *J. Am. Chem. Soc.* **102**, 6820–6824.
- Lamb, J. D., Izatt, R. M., Garrick, D. G., Bradshaw, J. S. & Christensen, J. J. (1981). *J. Membrane Sci.* **9**, 83–107.
- Lehn, J. M. & Sauvage, J. P. (1971). *J. Chem. Soc. Chem. Commun.* pp. 440–441.
- Metz, B., Moras, D. & Weiss, R. (1971). *Chem. Commun.* **286**, 444–445.
- Metz, B., Moras, D. & Weiss, R. (1976). *J. Chem. Soc. Perkin Trans.* pp. 423–429.
- Moore, A., Ricard, L., Le Floch, P. & Mezailles, N. (2003). *Organomet.* **22**, 1960–1966.
- Moras, D. & Weiss, R. (1973a). *Acta Cryst.* **B29**, 383–388.
- Moras, D. & Weiss, R. (1973b). *Acta Cryst.* **B29**, 396–399.
- Palacios, E., Burriel, R. & Ferloni, P. (2003). *Acta Cryst.* **B59**, 625–633.
- Riddell, F. G. (1992). *Chem. Br.* **28**, 533–535.
- Shannon, R. D. (1976). *Acta Cryst.* **32**, 751–767.
- Sheldrick, G. M. (2005). *CELL\_NOW*. University of Göttingen, Germany.
- Slosarek, G., Kozak, M., Gierszewski, J. & Pietraszko, A. (2006). *Acta Cryst.* **B62**, 102–108.
- Spek, A. L. (2003). *J. Appl. Cryst.* **36**, 7–13.
- Tirla, C., Mezailles, N., Ricard, L., Mathey, F. & Le Floch, P. (2002). *Inorg. Chem.* **41**, 6032–6037.
- Troxler, L. & Wipff, G. (1994). *J. Am. Chem. Soc.* **116**, 1468–1480.
- Varga, L. P., Sztanyik, L. B., Ronai, E., Bodo, K., Brucher, E., Gyori, B., Emri, J. & Kovacs, Z. (1994). *Int. J. Radiat. Biol.* **66**, 399–405.